Nonlinear Photoluminescence Spectroscopy of Carbon Nanotubes with Localized Exciton States

Munechiyo Iwamura, Naoto Akizuki, Yuhei Miyauchi, Shinichiro Mouri, Jonah Shaver, Zhenghong Gao, Laurent Cognet, Brahim Lounis, Kazunari Matsuda

Nonlinear photoluminescence spectroscopy of carbon nanotubes with localized exciton states

Munechiyo Iwamura[1], *Naoto Akizuki*[1], *Yuhei Miyauchi*[1,2,3]*, *Shinichiro Mouri*[1], *Jonah Shaver*[4], *Zhenghong Gao*[4], *Laurent Cognet*[4], *Brahim Lounis*[4], *and Kazunari Matsuda*[1]†

[1]Institute of Advanced Energy, Kyoto University, Uji, Kyoto 611-0011, Japan

[2]Japan Science and Technology Agency, PRESTO, 4-1-8 Honcho Kawaguchi, Saitama 332-0012, Japan

[3]Graduate School of Science, Nagoya University, Chikusa, Nagoya 464-8601, Japan

[4]Laboratoire Photonique Numérique et Nanosciences, Université de Bordeaux, Institut d'Optique Graduate School & CNRS, 351 cours de la libération, 33405 Talence, France

*miyauchi@iae.kyoto-u.ac.jp

†matsuda@iae.kyoto-u.ac.jp

KEYWORDS

carbon nanotube, nonlinear, photoluminescence, exciton, localized

ABSTRACT

We report distinctive nonlinear behavior of photoluminescence (PL) intensities from localized exciton states embedded in single-walled carbon nanotubes (SWNTs) at room temperature. We

found that PL from the local states exhibits strong nonlinear behavior with increasing continuous-wave excitation power density, whereas free exciton PL shows only weak sublinear behavior. The strong saturation behavior was observed regardless of the origin of the local states, and found to be nearly independent of the local state density. These results indicate that the strong PL nonlinearity arises from an universal mechanism to SWNTs with sparse local states. The significant nonlinear PL is attributed to rapid ground-state depletion of the local states caused by an efficient accumulation of photogenerated free excitons into the sparse local states through one-dimensional diffusional migration of excitons along nanotube axis; this mechanism is verified by Monte Carlo simulations of exciton diffusion dynamics.

Table of Contents Figure

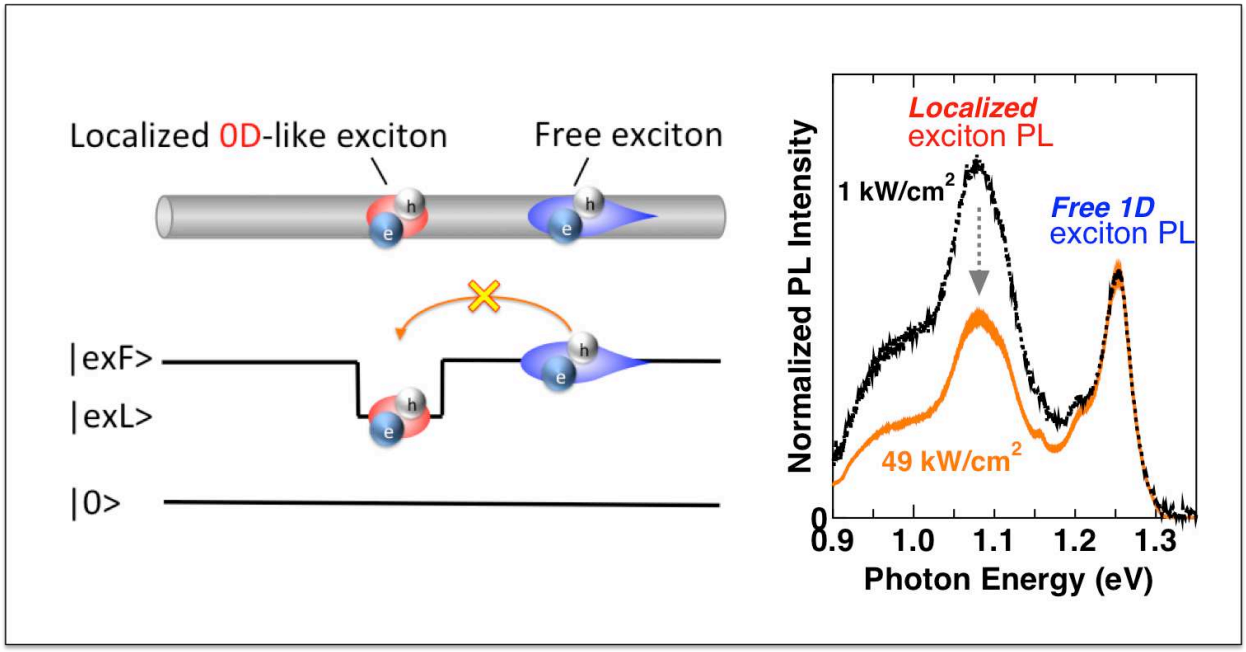

Because of the characteristic optical properties originating from their nearly ideal one-dimensional (1D) structures, single-walled carbon nanotubes (SWNTs) have been of great interest, not only for exploring fundamental photophysics in 1D systems but also for use in a variety of photonic applications including light-emitting diodes,[1, 2] single-photon sources,[3] solar cells,[4] and luminescent probes for bioimaging.[5] The optically excited electrons and holes in 1D SWNTs form bound states called excitons.[6-11] Quasi-1D excitons, especially in semiconducting SWNTs, have extremely large binding energies that dominate their optical properties even at room temperature.[9, 10] To date, various studies have been conducted on the fundamental properties of excitons in SWNTs such as excitonic fine structures,[11-13] exciton size,[14] radiative lifetimes,[15-19] absorption cross sections, [20-26] and formation of exciton complexes.[27-34] Moreover, 1D diffusion dynamics of excitons along SWNTs have been intensively studied; for example, details have been clarified concerning diffusion-limited luminescence quantum yields[16, 35-38] and nonlinear photoluminescence (PL) caused by rapid exciton–exciton annihilation (EEA) under intense photoexcitation.[39-44]

In addition to the intensive studies on intrinsic 1D exciton photophysics in SWNTs over the past decade, there have been rapidly growing interests in the impact of local electronic states on the optical properties of SWNTs.[3, 45-54] If well-organized local states are embedded in an intrinsic SWNT, the resulting complex nanostructure could be viewed as an unprecedented, nearly ideal 0D-1D hybrid low-dimensional system from which novel exciton photophysics may emerge.[51-54] Moreover, modifications originating from the additional local states may exert changes on the intrinsic optical properties of SWNTs that are favorable for novel optoelectronic applications. Hence, it is important to clarify the detailed exciton photophysics in such hybrid low-dimensional nanostructures.

Here we report on studies of photoluminescence (PL) intensities from localized exciton states generated by doping of atomic oxygen[47] and sp^3-defect[54] in SWNTs with increasing continuous-wave (cw) optical excitation power at room temperature. Strong nonlinear behavior of PL intensity from the local states was observed regardless of the origin of the local states, whereas the free-exciton PL exhibited only weak sublinear behavior. We also found that the PL saturation behavior of the local states merely depends on the density of these states in SWNTs. The distinctive difference in the PL saturation behavior between localized (0D-like) and free (1D)

exciton states can be reproduced by Monte Carlo simulations that consider exciton diffusion dynamics and ground-state depletion (state filling) at 0D-like local states. Comparisons of experimental and simulation results suggest that ground-state depletion, which causes PL saturation of the local states, originates from excitons photogenerated in intrinsic 1D segments being efficiently accumulated into a very small number of local states. The results of the simulations also imply that population inversion necessary for lasing, which has been hampered in intrinsic SWNTs owing to rapid EEA processes, may be achieved by using the luminescent local states in SWNTs even at relatively low power excitation conditions.

RESULTS AND DISCUSSION

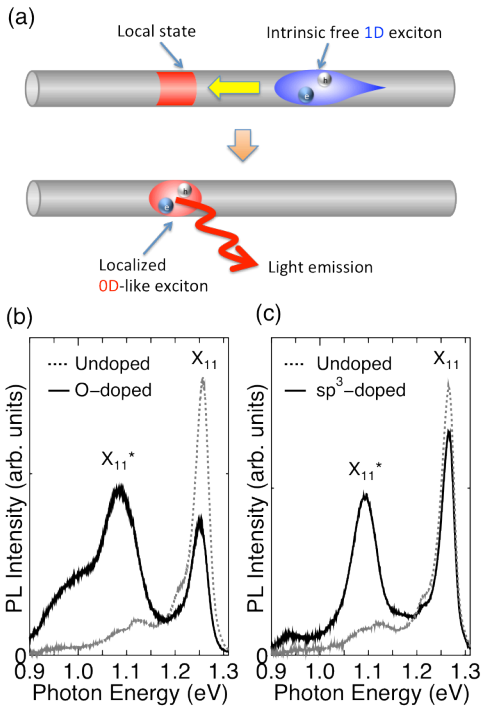

Figure 1. (a) Schematic of exciton dynamics in a SWNT with a 0D-like local luminescent state. Intrinsic free 1D exciton diffusively moves along the nanotube axis, converted to a 0D-like exciton at the local state, and emit brighter PL than 1D excitons. (b, c) PL spectra of SWNTs measured with an excitation photon energy of 2.18 eV before (dotted curve) and after (solid curve) the doping of (b) oxygen and (c) sp^3-defect, respectively. The dominant peak at ~1.25 eV (E_{11}) corresponds to PL from the intrinsic first subband excitons (X_{11}) in (6,5) SWNTs. The new peaks at ~1.05-1.10 eV (E_{11}*) in (b) and (c) are attributed to PL from the 0D-like excitons (X_{11}*) trapped at local quantum states embedded in SWNTs.

Figure 1(a) shows a schematic of exciton dynamics in SWNTs with luminescent local 0D-like states. Intrinsic free exciton diffusively moves along the 1D axis of SWNTs. 0D-like local luminescent states capture free 1D excitons, and convert them to 0D-like excitons that emit PL more efficiently than the free 1D excitons. Figures 1(b) and 1(c) show PL spectra of SWNTs before and after the oxygen-[47] and sp^3-defect[54] doping treatments to embed local luminescent states in SWNTs according to the procedures originally developed by Ghosh *et al.*,[47] and Piao *et al.*,[54] respectively (See Methods). These PL spectra were measured under low-power cw excitation (1.476 eV), which was low enough to avoid PL saturation. The dominant PL peak at an emission photon energy of ~1.25 eV (E_{11}) corresponds to radiative recombination of the first subband excitons (X_{11}) in (6,5) SWNTs. The new PL peaks at the emission photon energy of ~1.07 eV (E_{11}*) appears after the oxygen- and sp^3-defect doping treatments [Fig. 1(b) and 1(c)]. These new peaks have been attributed to PL emission from excitons trapped by local states generated by oxygen-[47] and sp^3-defect[54] doping in SWNTs on the basis of calculations using density functional theory[47, 54], respectively. The localized (0D-like) nature of the excitons responsible for the new peaks in oxygen-doped SWNTs has been also verified by temperature-dependent PL studies.[52] Hereafter, we refer to these localized excitonic states as X_{11}*, regardless of their origins.

Figures 2(a) and 2(b) show the PL spectra of oxygen- and sp^3-defect-doped SWNTs under cw excitation power densities from 1 to 49 kW/cm^2. PL intensities of each spectrum are divided by the corresponding excitation power density for comparison. The incident photon energy of 1.476 eV used for the measurements is nearly resonant with the E_{11} phonon sideband of (6, 5) SWNTs.[55-57] The PL intensities from X_{11} and X_{11}* states exhibit considerably different nonlinear behavior. The ratio of PL intensities of the intrinsic 1D state (X_{11}) and the local state (X_{11}*) clearly changes under strong excitation conditions; this indicates much stronger nonlinearity of the PL intensity from local states (X_{11}*) than from intrinsic 1D states (X_{11}) as the cw excitation power density is increased.

The integrated PL intensities (I_{11} and I_{11}*) from the intrinsic 1D states (X_{11}) and local states (X_{11}*) in oxygen- and sp^3-defect-doped SWNTs are plotted as functions of excitation power density in Fig. 2(c) and 2(d). I_{11} and I_{11}* were obtained by fits to the respective PL spectra. Both I_{11} and I_{11}* are normalized by the weak excitation power density of 1 kW/cm^2, where the PL

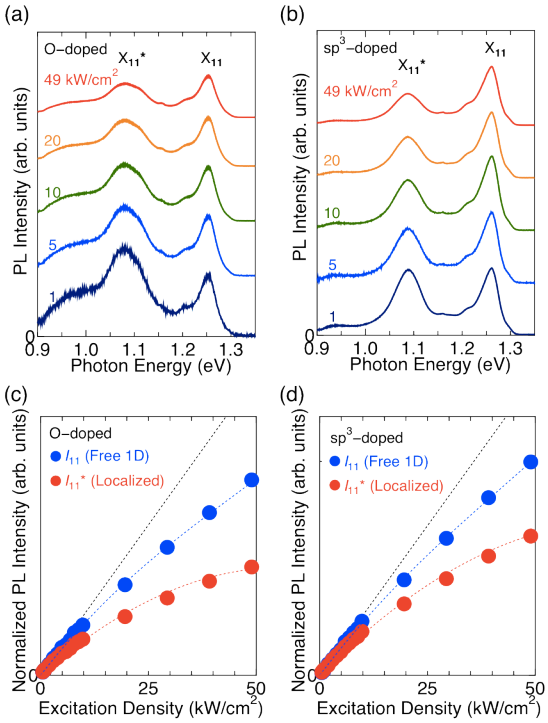

Figure 2. (a, b) Normalized PL spectra of (a) oxygen-doped and (b) sp^3-doped SWNTs taken at selected cw excitation power densities with an excitation photon energy of 1.476eV. Each spectrum is normalized by the corresponding excitation power density. It is clearly seen that the intensity ratio of X_{11}* and X_{11} peak heights depends on the excitation power density. (c, d) Normalized PL intensities as functions of cw excitation power density. Solid circles represent experimental data for the integrated intensities of X_{11}* PL peaks (I_{11}*, red solid circles) and X_{11} peaks (I_{11}, blue solid circles). Dashed curves are eye guides.

intensities are almost linear with respect to excitation density. The figure shows that there is a considerable difference between the nonlinear saturation behaviors of I_{11} and I_{11}* for both oxygen- and sp^3-defect-doped SWNTs. A similar effect has been reported for localized excitons in individual SWNTs at cryogenic temperature.[51, 58] Note that the nonlinear saturation behaviors for X_{11} and X_{11}* excitons in the both SWNTs are quite similar to each other regardless of the origin of the local states; this strongly suggests that there is a common physical mechanism for the observed strong PL nonlinearity that is related to unique exciton dynamics in SWNTs with 0D-like local states.

We further examined the nonlinear PL behavior of SWNTs with different local-state densities. Figure 3(a) compares PL spectra of various oxygen-doped SWNTs; each spectrum exhibits a

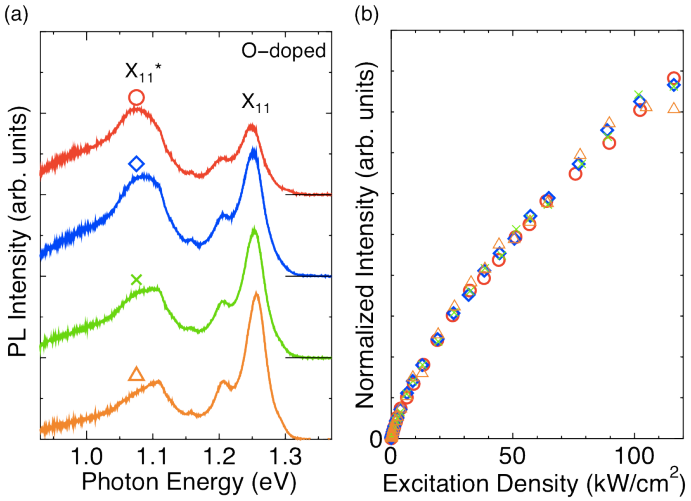

Figure 3. (a) PL spectra of oxygen-doped SWNTs prepared using four different ozone concentrations. Open symbols indicate each sample. Intensity ratio of X_{11}* and X_{11} PL varies depending on the sample reflecting different density of the local luminescent states embedded in the SWNTs. The slight differences of the spectra around the X_{11} PL peak of oxygen-doped SWNTs in Fig. 2 and Fig. 3 are due to the use of different sample batches. (b) Integrated PL intensities of X_{11}* peaks as functions of cw excitation power density, where the corresponding data are indicated by the same symbols used in (a).

different I_{11}* intensity that reflects different densities of the local states in the SWNTs (See Methods). These PL spectra were measured in the weak-excitation regime (1.3 kW/cm^2). Figure 3(b) compares the normalized PL intensities of I_{11}* in the various oxygen-doped SWNTs as functions of the excitation power density. We found no significant differences in the nonlinear behavior of I_{11}* in each sample. This suggests that the nonlinear PL behavior is nearly independent of the densities of local states within the range examined in this study.

To understand the mechanism of the strong nonlinear saturation behavior of I_{11}* from 0D-like local states in SWNTs regardless of the origin and density of the local states, we conducted computational simulations of exciton diffusion dynamics in SWNTs with 0D-like local states (See Methods). One of the important implications obtained from the simulation is the very small density of the luminescent local states in the 1D SWNTs. Figure 4 shows simulation results (solid curves) for various densities of local states (N_x) plotted together with typical experimental data for the nonlinear behavior of I_{11}* in oxygen-doped SWNTs. We found that the calculated

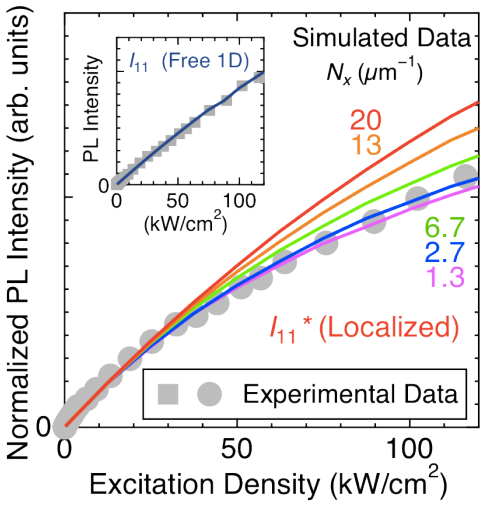

Figure 4. Calculated PL intensities as functions of cw excitation power density with densities of local states N_x from 1.3 to 20 μm^{-1}. Solid circles (solid squares in the inset) are typical experimental data of the X_{11}* (X_{11}) PL intensity I_{11}* (I_{11}) for oxygen-doped SWNTs. All calculated curves are normalized by the intensity at an excitation power density of 5 kW/cm^2. The experimental data for I_{11} in the inset is plotted with the calculated curve with N_x = 2.7 μm^{-1}.

saturation behaviors for small N_x (< ~5 μm^{-1}) are very similar to each other, whereas the calculations for larger N_x (> ~10 μm^{-1}) deviate considerably from the experimental values. The calculated N_x-dependent change in saturation behavior is reasonable, because the average exciton quenching site distance $1/n_q$ that corresponds to the effective nanotube length L^* in the simulation is ~150 nm (See Methods), and N_x < 5 μm^{-1} corresponds to less than one local state in L^*. In this case, the probability of having two or more local states in L^* is very small. Therefore, exciton dynamics near local states are nearly independent of N_x. In contrast, for N_x greater than ~10 μm^{-1}, the probability of having more than one local state in L^* increases with increasing N_x; thus, resulting in strong dependence of the saturation behavior on N_x. The experimental saturation curves are almost independent of the local state density as shown in Fig. 3, thereby confirming that N_x is very small (< 5 μm^{-1}) in the SWNTs examined in this study.

From these experimental and calculated results, the physical mechanism of the strong nonlinear PL behavior of X_{11}* excitons at the local states in SWNTs is understood as follows. First, incident photons are initially absorbed predominantly by intrinsic 1D SWNTs, and X_{11} excitons are generated. Then, the X_{11} excitons diffusively migrate along the intrinsic 1D parts of

the SWNTs, efficiently accumulate into sparsely distributed local states, and convert to localized (0D-like) X_{11}* excitons. In addition, the population decay of X_{11}* excitons at the local sites ($\sim 10^{-2}$ ps^{-1}) is slower than the diffusion-limited feed rate of X_{11} excitons to the X_{11}* states ($\sim 10^{-1}$ ps^{-1}).[52] Consequently, ground-state depletion (state filling) of 0D-like X_{11}* local states easily occurs; this results in the strong saturation of the PL intensities from the X_{11}* states.

The simulations further predict that local quantum states in SWNTs have quite favorable characteristics for optical applications. We found that the time-averaged number density of X_{11}* excitons can exceed $N_x/2$ at a X_{11} exciton cw photogeneration rate of less than 200 $ns^{-1}\mu m^{-1}$; this corresponds to a low cw excitation power density of less than 40 kW/cm^2 when E_{11} excitons are resonantly excited. The X_{11}* exciton number density of more than $N_x/2$ indicates that the number of excited states exceeds that of the ground state; namely, population inversions necessary for laser operations could occur at these local states. The optical gain threshold of individually dispersed SWNTs in a thin film has been previously reported to be 55 mJ/cm^2 by a two-nanosecond pulsed excitation at E_{22};[59] this corresponds to an effective cw excitation density of $\sim 3 \times 10^4$ kW/cm^2 for the pulse duration. Hence, an excitation density of 40 kW/cm^2 is surprisingly low. The availability of population inversion, even at low cw excitation conditions, originates from the same mechanism as that for strong nonlinear PL from the local states, namely, the efficient accumulation of excitons into local states. In contrast, at this low cw excitation condition, the time-averaged number density of intrinsic E_{11} excitons on an SWNT is found to be less than 0.3 $ns^{-1}\mu m^{-1}$, and most of the intrinsic part of the SWNT is in its ground state because of the extremely efficient nonradiative decay of excitons through EEA processes.[39-42, 44] The results of the simulations thus imply that lasing operations using SWNTs as gain media, which were heretofore hampered by very efficient EEA processes for the intrinsic 1D excitons in SWNTs, [39-42, 44] can be enabled using the local excitonic states embedded in SWNTs.

In conclusion, we have reported significant saturation behavior of the PL intensities from local electronic states generated by oxygen- and sp^3-defect-doping in SWNTs. The nonlinear behavior was found to be nearly independent of the origin and density of the local states. Computational simulations of the 1D exciton diffusion dynamics reproduce the experimental observations very well. The simulations suggest that the significant nonlinear behavior is dominated by ground-state depletion of local states, which originates from the efficient delivery of intrinsic 1D

excitons into the small number of local states. This universal exciton dynamics in SWNTs with sparse 0D-like local states is predicted to enable population inversion necessary for lasing in the local states in the relatively low-power cw optical excitation regime. These findings shed light on the possibility of novel optical applications of the local quantum states embedded in SWNTs, as well as the emergence of unique exciton photophysics in 1D-0D hybrid nanostructures.

METHODS

Sample preparation

Local electronic states in SWNTs were prepared by doping of atomic oxygen[47] or sp^3-defect[54] that induce local reduction of the band gap and exciton energy. The oxygen- and the sp^3-defect-doped SWNTs were, respectively, prepared using the procedure originally developed by Ghosh *et al.*[47] and Piao *et al*.[54] with some modifications in selections of chemicals and experimental parameters as described in Ref. 52. In short, (6,5)-rich CoMoCAT SWNTs purchased from Southwest Nanotechnologies (or purchased from Sigma Aldrich) were isolated by dispersion in D_2O with 0.2% (w/v) sodium dodecyl benzene sulfonate (SDBS), 60 (120) minutes of moderate bath sonication, 40 minutes of vigorous sonication with a tip-type sonicator, and centrifugation at an acceleration of 130 000 g for 4 (17) hours for the samples shown in Fig. 1 and 2 (Fig. 3 and 4). These experimental parameters were optimized for each sample batch of the CoMoCAT SWNTs. Slight differences of the PL spectra and nonlinear behavior shown in Fig. 2-4 could be because of the difference of the sample batches. For the oxygen-doping, the dispersion of isolated SWNTs was combined with a small amount of D_2O that contained dissolved ozone, and was left under the illumination of a desk lamp (~5 mW/cm^2) overnight; this enabled the moderate atomic oxygen doping to generate sparse oxygen-derived local states. For the sp^3-defect doping, the dispersion of isolated SWNTs was combined with a small amount of D_2O that contained dissolved organic diazonium salts,[54] and left under dark for more than 10 days; this enabled the moderate sp^3-defect doping to generate sparse sp^3-defect-derived local states.

Optical measurements

The excitation source for measurements of PL nonlinearity was a cw laser (Ti: Al_2O_3) with an 840-nm wavelength (1.476 eV) focused on the sample with a spot size of 4-6 μm. The PL from the sample was collected by an achromatic lens and passed through a confocal optical arrangement. Finally, the PL was recorded with a liquid-nitrogen-cooled InGaAs 1D array detector.

Monte Carlo simulations of exciton dynamics

We conducted computational simulations of the exciton diffusion dynamics in a hybrid-dimensional exciton system based on the Monte Carlo method.[37, 43, 60, 61] In the Monte Carlo simulations, the motion of an exciton in a SWNT is treated as a random walk. We consider 1D exciton diffusional-contact-quenching[16, 37] as the dominant exciton relaxation mechanism in an SWNT: if the exciton reaches nonradiative sites in the SWNT, it instantaneously disappears from the system. Here, nanotube ends are included as nonradiative sites as well as other local exciton quenching sites on the nanotube wall originating from structural defects, electronic impurity, or unintentional chemical attack.[16, 35-37, 62-66] An SWNT with an exciton-quenching site density n_d (including nanotube ends as exciton-quenching sites) corresponds to a nanotube in the simulation with an effective length $L^* = 1/n_d$. The length L^* (= $1/n_d$) is the substantial length within which excitons can migrate, and generally shorter than the actual length of SWNTs and intrinsic exciton diffusion length limited by radiative recombination processes.

At the beginning of a simulation, luminescent local states in SWNTs are randomly prepared so that the average density of the local states becomes N_x μm^{-1}. Then, the excitons are stochastically and spatially created according to the probability proportional to the excitation power at each unit time step. In the simulations, the same absorption cross sections per carbon atom were assumed for the 1D part and local states. This assumption is valid as far as the rate of direct photoexcitation of the local states is substantially smaller than that of indirect excitation through diffusion limited feeding of excitons; the fact that the PL excitation spectra probed at the X_{11} and X_{11}* emission photon energies are quite similar to each other[52] suggests that most of the X_{11}* excitons in the local states are generated originally in the 1D part of the SWNTs. In each unit time step δt, an intrinsic exciton randomly walks a characteristic distance δx. Considering

the 1D diffusion of a particle with diffusion constant D, the relationship $(\delta x)^2 = 2D\delta t$ is obtained. The time step δt corresponds to the exciton scattering time and is deduced to be 0.1 ps based on the homogeneous linewidth of Γ~13 meV[67] and the relationship $\Gamma = 2\hbar / \delta t$. Then, considering the relationship between the PL quantum yield η and D,[37] we find that $L^*/\delta x$ is the dimensionless parameter that determines η. The value $L^*/\delta x = 30$ is deduced from η ~1% with an exciton radiative lifetime of 1.6 ns[16] for (6,5) SWNTs dispersed in aqueous solution. Assuming that δx corresponds to an exciton coherence length[15, 68] on the order of ~5 nm, L^* ~ 150 nm is estimated.

In the simulations, if two excitons overlap at the same segment, exciton–exciton annihilation (EEA) takes place[39-44] instantaneously and only one exciton remains. The local luminescent state is treated as a two-level quantum system similar to an impurity bound 0D-like state in a semiconductor in which once an exciton is trapped at a local state another exciton cannot be trapped at the same local state due to the state-filling effect. Formation of exciton complexes such as biexcitons[30] is neglected. If an exciton reaches a local state with a density of N_x μm^{-1}, it is immediately captured by the local state. The localized exciton is subsequently eliminated from the system with a probability of τ^{-1} that corresponds to the sum of the radiative and nonradiative relaxation probabilities of the exciton being captured at a local site during each time step. The value τ = 70 ps was found to reproduce the experimental nonlinear PL behavior shown in Fig. 4 and was used in the simulations. This value of the lifetime is in good agreement with the experimental observation of τ ~ 95 ps.[52] From the time-averaged number of 1D intrinsic (X_{11}) and 0D-like (X_{11}*) localized excitons, the relative steady-state PL intensities from X_{11} and X_{11}* states, I_{11} and I_{11}*, could be calculated as functions of the cw excitation power density.

Solid curves in Fig. 4 are the results of Monte Carlo simulations of the nonlinear PL intensities from X_{11} (I_{11}, inset) and X_{11}* (I_{11}*) states as functions of excitation power density, where the density of the local (0D) state N_x = ~1-3 μm^{-1} and an absorption cross-section σ = 57 $nm^2/\mu m$ at 1.476 eV were found to reproduce the experimental curves very well. The simulations consistently reproduce the nonlinear saturation behavior of intrinsic (X_{11}) and localized (X_{11}*) excitons; this suggests that the saturation mechanism used in the simulations explains the exciton dynamics in SWNTs with 0D-like local states. The absorption cross-section of 57 $nm^2/\mu m$ at 1.476 eV corresponds to ~1.5 × 10^{-17} cm^2 per carbon atom at the E_{22} resonance (~2.2 eV)

considering the energy-dependent variation in the absorbance probed by PLE spectroscopy. This value is consistent with previously reported values that are on the order of 10^{-17} cm^2 per carbon atom in a single nanotube at E_{22} resonance,[20-25] and thus, supports the validity of the simulation.

ACKNOWLEDGMENT

Part of this work was supported by T. Umeyama, T. Murakami, and H. Imahori for experimental equipment. This study was supported by a Grant-in-Aid for Scientific Research (Nos. 24681031, 22740195, 22016007, and 23340085), Yamada Science Foundation, and by PRESTO from JST.

REFERENCES

1. Misewich, J. A.; Martel, R.; Avouris, P.; Tsang, J. C.; Heinze, S.; Tersoff, J. Electrically Induced Optical Emission from a Carbon Nanotube FET. *Science* **2003,** 300, (5620), 783-786.
2. Avouris, P.; Freitag, M.; Perebeinos, V. Carbon-nanotube Photonics and Optoelectronics. *Nature Photon.* **2008,** 2, (6), 341-350.
3. Högele, A.; Galland, C.; Winger, M.; Imamoğlu, A. Photon Antibunching in the Photoluminescence Spectra of a Single Carbon Nanotube. *Phys. Rev. Lett.* **2008,** 100, (21), 217401.
4. Jung, Y.; Li, X.; Rajan, N. K.; Taylor, A. D.; Reed, M. A. Record High Efficiency Single-Walled Carbon Nanotube/Silicon p–n Junction Solar Cells. *Nano Lett.* **2012,** 13, (1), 95-99.
5. Welsher, K.; Liu, Z.; Sherlock, S. P.; Robinson, J. T.; Chen, Z.; Daranciang, D.; Dai, H. A Route to Brightly Fluorescent Carbon Nanotubes for Near-infrared Imaging in Mice. *Nature Nanotech.* **2009,** 4, (11), 773-780.
6. Ando, T. Excitons in Carbon Nanotubes. *J. Phys. Soc. Jpn.* **1997,** 66, (4), 1066-1073.
7. Spataru, C. D.; Ismail-Beigi, S.; Benedict, L. X.; Louie, S. G. Excitonic Effects and Optical Spectra of Single-Walled Carbon Nanotubes. *Phys. Rev. Lett.* **2004,** 92, (7), 077402.
8. Perebeinos, V.; Tersoff, J.; Avouris, P. Scaling of Excitons in Carbon Nanotubes. *Phys. Rev. Lett.* **2004,** 92, (25), 257402.
9. Wang, F.; Dukovic, G.; Brus, L. E.; Heinz, T. F. The Optical Resonances in Carbon Nanotubes Arise from Excitons. *Science* **2005,** 308, (5723), 838-841.
10. Maultzsch, J.; Pomraenke, R.; Reich, S.; Chang, E.; Prezzi, D.; Ruini, A.; Molinari, E.; Strano, M. S.; Thomsen, C.; Lienau, C. Exciton Binding Energies in Carbon Nanotubes From Two-photon Photoluminescence. *Phys. Rev. B* **2005,** 72, (24), 241402(R).
11. Zhao, H.; Mazumdar, S. Electron-Electron Interaction Effects on the Optical Excitations of Semiconducting Single-Walled Carbon Nanotubes. *Phys. Rev. Lett.* **2004,** 93, (15), 157402.
12. Matsunaga, R.; Matsuda, K.; Kanemitsu, Y. Evidence for Dark Excitons in a Single Carbon Nanotube due to the Aharonov-Bohm Effect. *Phys. Rev. Lett.* **2008,** 101, (14), 147404.

13. Srivastava, A.; Htoon, H.; Klimov, V. I.; Kono, J. Direct Observation of Dark Excitons in Individual Carbon Nanotubes: Inhomogeneity in the Exchange Splitting. *Phys. Rev. Lett.* **2008,** 101, (8), 087402.
14. Lüer, L.; Hoseinkhani, S.; Polli, D.; Crochet, J.; Hertel, T.; Lanzani, G. Size and mobility of excitons in (6, 5) carbon nanotubes. *Nature Phys.* **2009,** 5, (1), 54-58.
15. Miyauchi, Y.; Hirori, H.; Matsuda, K.; Kanemitsu, Y. Radiative Lifetimes and Coherence Lengths of One-dimensional Excitons in Single-walled Carbon Nanotubes. *Phys. Rev. B* **2009,** 80, (8), 081410(R).
16. Hertel, T.; Himmelein, S.; Ackermann, T.; Stich, D.; Crochet, J. Diffusion Limited Photoluminescence Quantum Yields in 1-D Semiconductors: Single-Wall Carbon Nanotubes. *ACS Nano* **2010,** 4, (12), 7161-7168.
17. Wang, F.; Dukovic, G.; Brus, L. E.; Heinz, T. F. Time-Resolved Fluorescence of Carbon Nanotubes and Its Implication for Radiative Lifetimes. *Phys. Rev. Lett.* **2004,** 92, (17), 177401.
18. Spataru, C. D.; Ismail-Beigi, S.; Capaz, R. B.; Louie, S. G. Theory and Ab Initio Calculation of Radiative Lifetime of Excitons in Semiconducting Carbon Nanotubes. *Phys. Rev. Lett.* **2005,** 95, (24), 247402.
19. Perebeinos, V.; Tersoff, J.; Avouris, P. Radiative Lifetime of Excitons in Carbon Nanotubes. *Nano Lett.* **2005,** 5, (12), 2495-2499.
20. Berciaud, S.; Cognet, L.; Lounis, B. Luminescence Decay and the Absorption Cross Section of Individual Single-Walled Carbon Nanotubes. *Phys. Rev. Lett.* **2008,** 101, (7), 077402.
21. Schöppler, F.; Mann, C.; Hain, T. C.; Neubauer, F. M.; Privitera, G.; Bonaccorso, F.; Chu, D.; Ferrari, A. C.; Hertel, T. Molar Extinction Coefficient of Single-Wall Carbon Nanotubes. *J. Phys. Chem. C* **2011,** 115, (30), 14682-14686.
22. Koyama, T.; Miyata, Y.; Kishida, H.; Shinohara, H.; Nakamura, A. Photophysics in Single-Walled Carbon Nanotubes with (6,4) Chirality at High Excitation Densities: Bimolecular Auger Recombination and Phase-Space Filling of Excitons. *J. Phys. Chem. C* **2013,** 117, (4), 1974-1981.
23. Joh, D. Y.; Kinder, J.; Herman, L. H.; Ju, S.-Y.; Segal, M. A.; Johnson, J. N.; ChanGarnet, K. L.; Park, J. Single-walled Carbon Nanotubes as Excitonic Optical Wires. *Nature Nanotech.* **2010,** 6, (1), 51-56.
24. Oudjedi, L.; Parra-Vasquez, A. N. G.; Godin, A. G.; Cognet, L.; Lounis, B. Metrological Investigation of the (6,5) Carbon Nanotube Absorption Cross Section. *J. Phys. Chem. Lett.* **2013,** 4, (9), 1460-1464.
25. Streit, J. K.; Bachilo, S. M.; Ghosh, S.; Lin, C.-W.; Weisman, R. B. Directly Measured Optical Absorption Cross Sections for Structure-Selected Single-Walled Carbon Nanotubes. *Nano Lett.* **2014,** 14, (3), 1530-1536.
26. Kumamoto, Y.; Yoshida, M.; Ishii, A.; Yokoyama, A.; Shimada, T.; Kato, Y. K. Spontaneous Exciton Dissociation in Carbon Nanotubes. *Phys. Rev. Lett.* **2014,** 112, (11), 117401.
27. Matsunaga, R.; Matsuda, K.; Kanemitsu, Y. Observation of Charged Excitons in Hole-Doped Carbon Nanotubes Using Photoluminescence and Absorption Spectroscopy. *Phys. Rev. Lett.* **2011,** 106, (3), 037404.
28. Santos, S. M.; Yuma, B.; Berciaud, S.; Shaver, J.; Gallart, M.; Gilliot, P.; Cognet, L.; Lounis, B. All-Optical Trion Generation in Single-Walled Carbon Nanotubes. *Phys. Rev. Lett.* **2011,** 107, (18), 187401.

29. Park, J. S.; Hirana, Y.; Mouri, S.; Miyauchi, Y.; Nakashima, N.; Matsuda, K. Observation of Negative and Positive Trions in the Electrochemically Carrier-Doped Single-Walled Carbon Nanotubes. *J. Am. Chem. Soc.* **2012,** 134, (35), 14461-14466.
30. Colombier, L.; Selles, J.; Rousseau, E.; Lauret, J. S.; Vialla, F.; Voisin, C.; Cassabois, G. Detection of a Biexciton in Semiconducting Carbon Nanotubes Using Nonlinear Optical Spectroscopy. *Phys. Rev. Lett.* **2012,** 109, (19), 197402.
31. Yuma, B.; Berciaud, S.; Besbas, J.; Shaver, J.; Santos, S.; Ghosh, S.; Weisman, R. B.; Cognet, L.; Gallart, M.; Ziegler, M.; Hönerlage, B.; Lounis, B.; Gilliot, P. Biexciton, Single Carrier, and Trion Generation Dynamics in Single-walled Carbon Nanotubes. *Phys. Rev. B* **2013,** 87, (20), 205412.
32. Koyama, T.; Shimizu, S.; Miyata, Y.; Shinohara, H.; Nakamura, A. Ultrafast Formation and Decay Dynamics of Trions in p-doped Single-walled Carbon Nanotubes. *Phys. Rev. B* **2013,** 87, (16), 165430.
33. Nishihara, T.; Yamada, Y.; Kanemitsu, Y. Dynamics of Exciton-hole Recombination in Hole-doped Single-walled Carbon Nanotubes. *Phys. Rev. B* **2012,** 86, (7), 075449.
34. Mouri, S.; Miyauchi, Y.; Iwamura, M.; Matsuda, K. Temperature Dependence of Photoluminescence Spectra in Hole-doped Single-walled Carbon Nanotubes: Implications of Trion Localization. *Phys. Rev. B* **2013,** 87, (4), 045408.
35. Cognet, L.; Tsyboulski, D. A.; Rocha, J.-D. R.; Doyle, C. D.; Tour, J. M.; Weisman, R. B. Stepwise Quenching of Exciton Fluorescence in Carbon Nanotubes by Single-Molecule Reactions. *Science* **2007,** 316, (5830), 1465-1468.
36. Miyauchi, Y.; Matsuda, K.; Yamamoto, Y.; Nakashima, N.; Kanemitsu, Y. Length-Dependent Photoluminescence Lifetimes in Single-Walled Carbon Nanotubes. *J. Phys. Chem. C* **2010,** 114, (30), 12905-12908.
37. Harrah, D. M.; Swan, A. K. The Role of Length and Defects on Optical Quantum Efficiency and Exciton Decay Dynamics in Single-Walled Carbon Nanotubes. *ACS Nano* **2011,** 5, (1), 647-655.
38. Crochet, J. J.; Duque, J. G.; Werner, J. H.; Lounis, B.; Cognet, L.; Doorn, S. K. Disorder Limited Exciton Transport in Colloidal Single-Wall Carbon Nanotubes. *Nano Lett.* **2012,** 12, 5091-5096.
39. Wang, F.; Dukovic, G.; Knoesel, E.; Brus, L. E.; Heinz, T. F. Observation of Rapid Auger Recombination in Optically Excited Semiconducting Carbon Nanotubes. *Phys. Rev. B* **2004,** 70, (24), 241403(R).
40. Ma, Y.-Z.; Valkunas, L.; Dexheimer, S. L.; Bachilo, S. M.; Fleming, G. R. Femtosecond Spectroscopy of Optical Excitations in Single-Walled Carbon Nanotubes: Evidence for Exciton-Exciton Annihilation. *Phys. Rev. Lett.* **2005,** 94, (15), 157402.
41. Matsuda, K.; Inoue, T.; Murakami, Y.; Maruyama, S.; Kanemitsu, Y. Exciton Dephasing and Multiexciton Recombinations in a Single Carbon Nanotube. *Phys. Rev. B* **2008,** 77, (3), 033406.
42. Murakami, Y.; Kono, J. Nonlinear Photoluminescence Excitation Spectroscopy of Carbon Nanotubes: Exploring the Upper Density Limit of One-Dimensional Excitons. *Phys. Rev. Lett.* **2009,** 102, (3), 037401.
43. Srivastava, A.; Kono, J. Diffusion-limited Exciton-exciton Annihilation in Single-walled Carbon Nanotubes: A Time-Dependent Analysis. *Phys. Rev. B* **2009,** 79, (20), 205407.

44. Xiao, Y. F.; Nhan, T. Q.; Wilson, M. W. B.; Fraser, J. M. Saturation of the Photoluminescence at Few-Exciton Levels in a Single-Walled Carbon Nanotube under Ultrafast Excitation. *Phys. Rev. Lett.* **2010,** 104, (1), 017401.
45. Iakoubovskii, K.; Minami, N.; Kim, Y.; Miyashita, K.; Kazaoui, S.; Nalini, B. Midgap Luminescence Centers in Single-wall Carbon Nanotubes Created by Ultraviolet Illumination. *Appl. Phys. Lett.* **2006,** 89, (17), 173108.
46. McDonald, T. J.; Blackburn, J. L.; Metzger, W. K.; Rumbles, G.; Heben, M. J. Chiral-Selective Protection of Single-walled Carbon Nanotube Photoluminescence by Surfactant Selection. *J. Phys. Chem. C* **2007,** 111, (48), 17894-17900.
47. Ghosh, S.; Bachilo, S. M.; Simonette, R. A.; Beckingham, K. M.; Weisman, R. B. Oxygen Doping Modifies Near-Infrared Band Gaps in Fluorescent Single-Walled Carbon Nanotubes. *Science* **2010,** 330, (6011), 1656-1659.
48. Tomio, Y.; Suzuura, H. Impurity-induced Valley Mixing of Excitons in Semiconducting Carbon Nanotubes. *Physica E: Low-dimensional Systems and Nanostructures* **2010,** 42, (4), 783-786.
49. Kilina, S.; Ramirez, J.; Tretiak, S. Brightening of the Lowest Exciton in Carbon Nanotubes via Chemical Functionalization. *Nano Lett.* **2012,** 12, (5), 2306-2312.
50. Maeda, Y.; Higo, J.; Amagai, Y.; Matsui, J.; Ohkubo, K.; Yoshigoe, Y.; Hashimoto, M.; Eguchi, K.; Yamada, M.; Hasegawa, T.; Sato, Y.; Zhou, J.; Lu, J.; Miyashita, T.; Fukuzumi, S.; Murakami, T.; Tohji, K.; Nagase, S.; Akasaka, T. Helicity-Selective Photoreaction of Single-Walled Carbon Nanotubes with Organosulfur Compounds in the Presence of Oxygen. *J. Am. Chem. Soc.* **2013,** 135, (16), 6356-6362.
51. Hofmann, M. S.; Gluckert, J. T.; Noe, J.; Bourjau, C.; Dehmel, R.; Högele, A. Bright, Long-lived and Coherent Excitons in Carbon Nanotube Quantum Dots. *Nature Nanotech.* **2013,** 8, (7), 502-505.
52. Miyauchi, Y.; Iwamura, M.; Mouri, S.; Kawazoe, T.; Ohtsu, M.; Matsuda, K. Brightening of excitons in carbon nanotubes on dimensionality modification. *Nature Photon.* **2013,** 7, (9), 715-719.
53. Sarpkaya, I.; Zhang, Z.; Walden-Newman, W.; Wang, X.; Hone, J.; Wong, C. W.; Strauf, S. Prolonged Spontaneous Emission and Dephasing of Localized Excitons in Air-bridged Carbon Nanotubes. *Nat. Commun.* **2013,** 4, 2152.
54. Piao, Y.; Meany, B.; Powell, L. R.; Valley, N.; Kwon, H.; Schatz, G. C.; Wang, Y. Brightening of Carbon Nanotube Photoluminescence through the Incorporation of sp^3 defects. *Nature Chem.* **2013,** 5, (10), 840-845.
55. Miyauchi, Y.; Maruyama, S. Identification of an Excitonic Phonon Sideband by Photoluminescence Spectroscopy of Single-walled Carbon-13 Nanotubes. *Phys. Rev. B* **2006,** 74, (3), 035415.
56. Plentz, F.; Ribeiro, H. B.; Jorio, A.; Strano, M. S.; Pimenta, M. A. Direct Experimental Evidence of Exciton-Phonon Bound States in Carbon Nanotubes. *Phys. Rev. Lett.* **2005,** 95, (24), 247401.
57. Htoon, H.; O'Connell, M. J.; Doorn, S. K.; Klimov, V. I. Single Carbon Nanotubes Probed by Photoluminescence Excitation Spectroscopy: The Role of Phonon-Assisted Transitions. *Phys. Rev. Lett.* **2005,** 94, (12), 127403.
58. Hagen, A.; Steiner, M.; Raschke, M. B.; Lienau, C.; Hertel, T.; Qian, H.; Meixner, A. J.; Hartschuh, A. Exponential Decay Lifetimes of Excitons in Individual Single-Walled Carbon Nanotubes. *Phys. Rev. Lett.* **2005,** 95, (19), 197401.

59. Gaufres, E.; Izard, N.; Le Roux, X.; Marris-Morini, D.; Kazaoui, S.; Cassan, E.; Vivien, L. Optical Gain in Carbon Nanotubes. *Appl. Phys. Lett.* **2010,** 96, (23), 231105.
60. Murakami, Y.; Kono, J. Existence of an Upper Limit on the Density of Excitons in Carbon Nanotubes by Diffusion-limited Exciton-exciton Annihilation: Experiment and Theory. *Phys. Rev. B* **2009,** 80, (3), 035432.
61. Santos, S. M. Optical Spectroscopy of Bound Excitonic States in Single Walled Carbon Nanotubes. **2012**, Ph.D Thesis, l'Université de Bordeaux 1.
62. Crochet, J. J.; Duque, J. G.; Werner, J. H.; Doorn, S. K. Photoluminescence Imaging of Electronic-impurity-induced Exciton Quenching in Single-walled Carbon Nanotubes. *Nature Nanotech.* **2012,** 7, (2), 126-132.
63. Ju, S.-Y.; Kopcha, W. P.; Papadimitrakopoulos, F. Brightly Fluorescent Single-Walled Carbon Nanotubes via an Oxygen-Excluding Surfactant Organization. *Science* **2009,** 323, (5919), 1319-1323.
64. Lee, A. J.; Wang, X.; Carlson, L. J.; Smyder, J. A.; Loesch, B.; Tu, X.; Zheng, M.; Krauss, T. D. Bright Fluorescence from Individual Single-Walled Carbon Nanotubes. *Nano Lett.* **2011,** 11, (4), 1636-1640.
65. Rajan, A.; Strano, M. S.; Heller, D. A.; Hertel, T.; Schulten, K. Length-Dependent Optical Effects in Single Walled Carbon Nanotubes. *J. Phys. Chem. B* **2008,** 112, (19), 6211-6213.
66. Georgi, C.; Böhmler, M.; Qian, H.; Novotny, L.; Hartschuh, A. Probing Exciton Propagation and Quenching in Carbon Nanotubes with Near-field Optical Microscopy. *phys. stat. sol. b* **2009,** 246, (11-12), 2683-2688.
67. Yoshikawa, K.; Matsunaga, R.; Matsuda, K.; Kanemitsu, Y. Mechanism of Exciton Dephasing in a Single Carbon Nanotube Studied by Photoluminescence Spectroscopy. *Appl. Phys. Lett.* **2009,** 94, (9), 093109.
68. Song, D.; Wang, F.; Dukovic, G.; Zheng, M.; Semke, E. D.; Brus, L. E.; Heinz, T. F. Measurement of the Optical Stark Effect in Semiconducting Carbon Nanotubes. *Appl. Phys. A* **2009,** 96, 283-287.